# Aeroelastic Analysis of Mach 0.8 Transonic Truss-Braced Wing Aircraft

Juntao Xiong\*

KBR Wyle, Inc., Moffett Field, CA 94035

Nhan Nguyen†

NASA Ames Research Center, Moffett Field, CA 94035

Robert E. Bartels‡

NASA Langley Research Center, Hampton, VA 23681

This paper presents an aeroelastic analysis of the Mach 0.8 Transonic Truss-Braced Wing (TTBW) aircraft jig shape using an in-house developed tool based on VSPAERO. A vortex-lattice model of the Mach 0.8 TTBW model is developed, and a transonic and viscous flow correction method is implemented to account for transonic and viscous flow effects. A correction method for the wing-strut interference aerodynamics is developed and applied to the VSPAERO solver. The Galerkin method is used to calculate the geometry deformation under aerodynamic force. The aero-structural analysis solver VSPAERO coupled to the mode shapes computed by NASTRAN using the Galerkin method provides a rapid aircraft aero-structural analysis. A high-fidelity CFD solver FUN3D is used to verify the results. The aeroelastic simulation results show that the aeroelastic lift coefficient is reduced about  $0.05 \sim 0.07$ , drag polar is not affected by aeroelasticity, and the pitching moment is reduced about 30% at Mach 0.8 and altitude 40,000 ft.

#### I. Introduction

The Subsonic Ultra Green Aircraft Research (SUGAR) Transonic Truss-Braced Wing (TTBW) aircraft concept is a Boeing-developed N+3 aircraft configuration funded by NASA Aeronautics Research Mission Directorate (ARMD) Advanced Air Transport Technologies (AATT) project. 1,2,3 The TTBW aircraft concept is designed to be aerodynamically efficient by employing a wing aspect ratio of about 19.55, which is significantly greater than those of cantilever wing transport configurations. Without structural bracing, the increase in the wing root bending moment would require a significant structural reinforcement which would lead to an increase in the structural weight that would offset the aerodynamic benefit of the high aspect ratio wing. Thus, the design of a truss-braced structure is a Multidisciplinary Design Optimization (MDO) process that strives to achieve a delicate balance between aerodynamic efficiency and structural efficiency. A typical MDO process uses a variety of different tools of varying fidelity for many different purposes such as aerodynamic prediction, aero-structural analysis, flutter analysis. Computational Fluid Dynamics (CFD) is the main tool for aerodynamic prediction. On the other hand, for flight dynamic analysis of stability and control, a lower-order tool may be sufficient during the early stage of the design.

In SUGAR Phase IV, Boeing updated the TTBW concept to operate at a cruise Mach number 0.80 which is consistent with today's commercial transport aircraft.<sup>4</sup> Figure 1 illustrates the concept of the Mach 0.8 TTBW aircraft. To evaluate the aircraft performance and perform optimization of the Mach 0.8 TTBW aircraft, a fast and reliable aero-structure analysis model is desired. In this paper an aero-structure analysis model of the Mach 0.8 TTBW aircraft is developed using VSPAERO. The VSPAERO model of the Mach 0.8 TTBW includes the low-fidelity vortex-lattice model for steady-state aerodynamics. Transonic and viscous flow corrections for the steady-state aerodynamics are implemented using a transonic small disturbance (TSD) code called TSFOIL coupled to an in-house integral boundary layer (IBL) code. In the region near the strut attachment to the wing, the flow involves a considerable degree of interactions between the wing and the strut. A correction method based on a high-fidelity CFD solver FUN3D simulations for the wing-strut interference aerodynamics is developed and applied to the VSPAERO solver. The Galerkin method is used to calculate

<sup>\*</sup>Aerospace Engineer, Intelligent System Division, juntao.xiong@nasa.gov, AIAA Member

<sup>†</sup>Senior Research Scientist and Technical Group Lead, Intelligent Systems Division, nhan.t.nguyen@nasa.gov, Associate Fellow AIAA

<sup>\*</sup>Research Aerospace Engineer, NASA Langley Research Center, MS 340, robert.e.bartels@nasa.gov, AIAA Senior Member

the geometry deformation under aerodynamic force. The aero-structural analysis solver VSPAERO coupled to the mode shapes computed by NASTRAN using the Galerkin method provides a rapid aircraft aero-structural analysis for the Mach 0.8 TTBW aircraft jig shape. The high-fidelity CFD solver FUN3D is used to verify the results.



Figure 1 Boeing SUGAR Mach 0.8 Transonic Truss-Braced Wing (TTBW) Aircraft Concept

## II. Aerodynamic Model of the Truss-Braced Wing

#### A. VSPAERO Model

In order to develop a rapid aeroelastic analysis that facilitates a vehicle MDAO process, a lower-fidelity aerodynamic model of the TTBW is necessary. VSPAERO<sup>5</sup> is a solver that includes both the vortex lattice method and the full panel method based on generalized vortex rings. The core VSPAERO solver is based on an agglomerated multi-pole approach, coupled with a preconditioned linear solver, to reduce solution times. Adaptive wakes, time-accurate, unsteady analyses, and propeller modeling are all supported. VSPAERO is part of the OpenVSP design package and is freely available under the NASA open source license. Figure 2 illustrates the Mach 0.8 TTBW VSPAERO models. Figure 3 shows the differential pressure coefficient contour at Mach 0.8 and an angle of attack of 2° for the VSPAERO vortex-lattice model.



Figure 2 VSPAERO Model of Mach 0.8 TTBW

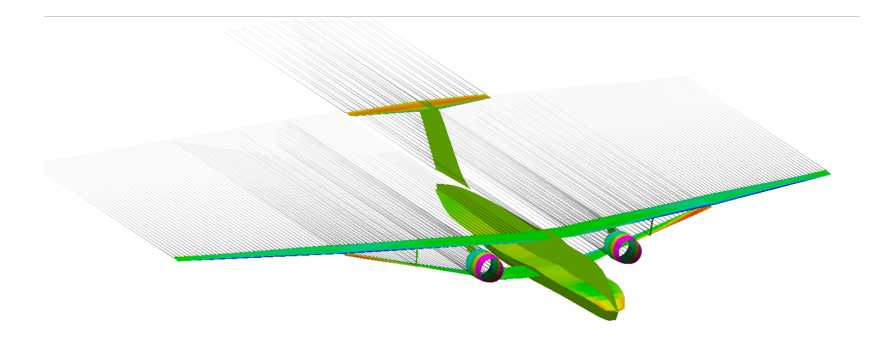


Figure 3 Differential Pressure Coefficient Contour of VSPAERO Model of Mach 0.8 TTBW

#### **B.** Transonic and Viscous Flow Correction

Because of the missing transonic effect in the linear potential flow method, a method for transonic and viscous corrections has recently been developed.<sup>6,7,8</sup> In this method, a full-configuration aerodynamic model can be based on the vortex-lattice or panel method. The wing is discretized into several spanwise sections at which the section lift coefficients computed by the potential flow method are used to correct for the transonic and viscous flow effects.<sup>7,8</sup> The transonic and viscous correction method is an iterative process to compute the incremental section lift coefficient due to transonic and viscous flow by a virtual re-twist of the individual wing sections to account for the accompanied change in the effective local angle of attack.<sup>8</sup> Implementation of the correction begins by initializing the virtual twist angle due to transonic and viscous corrections,  $\gamma(y)$ , to zero. The effective 2D angle of attack is then calculated for each airfoil using,

$$\alpha_{2D}(y) = \alpha_0(y) + \frac{c_{l_{3D}}(y)}{c_{l_{\alpha}}} - \gamma(y),$$
 (1)

where  $\alpha_{2D}$  is the effective airfoil angle of attack,  $\alpha_0$  is the airfoil zero-lift angle of attack,  $c_{l_{3D}}$  is the section lift coefficient obtained via VSPAERO, and  $c_{l_{\alpha}}$  is the 2D lift curve slope corrected for sweep as follows:

$$c_{l_{\alpha}} = \frac{2\pi}{\sqrt{1 - M_{\Lambda}^2}}. (2)$$

Here,  $M_{\Lambda}$  is the Mach number based on the mid-chord sweep angle. Each airfoil is analyzed by the TSD/IBL model at the effective angle of attack. The transonic flow correction is handled by the transonic small disturbance (TSD) code TSFOIL.<sup>9</sup> This code is loosely coupled to the in-house integral boundary layer (IBL) code developed by Nguyen et al.<sup>6</sup> to correct for the viscous flow interaction with the transonic shock on an airfoil. Optionally, the correction method can be performed using the 2D Euler CFD code MSES with an integral boundary layer method developed by Mark Drela<sup>10</sup> as an available option.. The virtual twist angle is then updated for each section according to:

$$\gamma_{i+1}(y) = \gamma_i(y) + \frac{c_{l_{2D_i}}(y) - c_{l_{3D_i}}(y)}{c_{l_{\alpha}}},$$
(3)

where  $c_{l_{2D_i}}$  corresponds to the airfoil lift coefficient calculated by TSFOIL or MSES for iteration i.

The coupling and iterative update process is repeated until the 3D wing section lift and the 2D airfoil lift computed by the TSD/IBL correction method converge for all sections. Wave and friction drag are calculated by the TSD/IBL correction method, whereas lift, pitching moment, and induced drag are calculated by the VSPAERO model. The

flow chart of the transonic and viscous flow correction method is shown in Figure 4.8 An extensive validation of the transonic and viscous flow correction method has been performed to compare the method against RANS CFD solvers. The solution method agrees quite well in terms of key aerodynamic parameters and pressure distribution results. The major advantage of using a potential flow method coupled to the transonic and viscous flow corrections is the computational efficiency of the method, which is several orders of magnitude faster than a typical RANS CFD solution. This computational efficiency becomes highly important when the potential flow solver is coupled to a structural finite-element model for aero-structural modeling analysis.

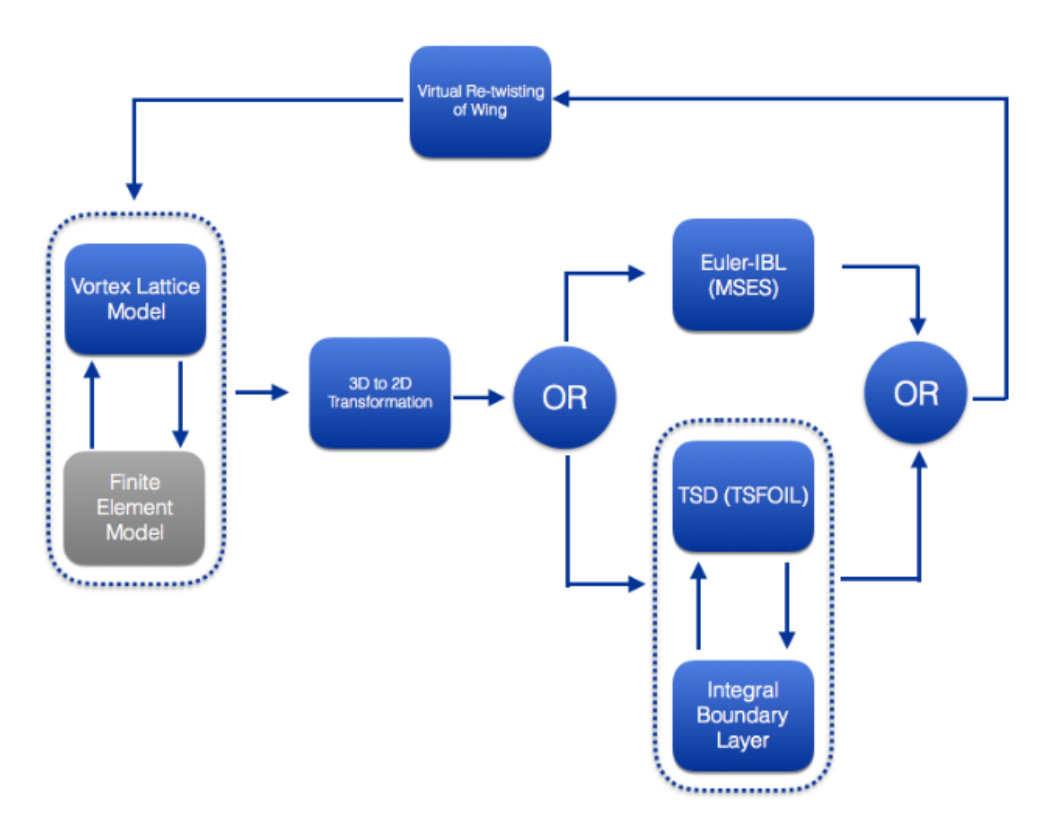


Figure 4 Transonic and Viscous Correction Flow Chart

## C. Wing-Strut Interference Aerodynamic Correction

The TTBW configuration is a complex geometry that includes a strut juncture region where the effect of interference aerodynamics can influence the overall aerodynamic performance of the aircraft. As the strut approaches the wing from below, the transonic and viscous flow corrections using the TSD/IBL method are no longer valid due to the interactions between the wing airfoil and strut airfoil. <sup>11,12</sup> To account for these interference aerodynamics, CFD models of the wing-strut configuration and the wing-alone configuration of the TTBW aircraft are developed using FUN3D. To isolate the interference aerodynamic effect for the wing and strut, the nacelle, the pylon, and the horizontal tail are removed from the models. Surface pressure coefficients are computed for both configurations at various wing stations. By comparing the wing-strut data to the wing-alone data, it is seen that the presence of the strut induces a suction peak along the lower surface of the wing near the wing-strut juncture. <sup>12</sup>

A wing-strut interference correction model for Mach 0.8 TTBW is developed to correct the VSPAERO model. <sup>13</sup> The correction method is applied to the VSPAERO+TSD/IBL model to update the section lift, drag, and pitching moment coefficient of each wing section.

The interference correction,  $\Delta c_{IC}$ , that is applied to the model is calculated using the following equation,

$$\Delta c_{IC} = \Delta c_{FUN3D} - \Delta c_{VSPAERO+TSD/IBL},\tag{4}$$

where c represents a key aerodynamic parameter such as  $c_l$ ,  $c_d$ , and  $c_m$  and  $\Delta$  represents the change in the given parameter between the wing-strut configuration and wing-alone configuration.

#### D. Aerodynamic Analysis of Cruise Shape Geometry

The VSPAERO model is used for the aerodynamic analysis of the cruise 1g shape TTBW geometry for the Mach 0.8 TTBW aircraft configuration.. Wind tunnel test data of the cruise shape geometry in NASA Ames 11-Ft Transonic Wind Tunnel are available for validation of the VSPAERO models. Figure 5 shows the plots of the lift and drag coefficients computed by VSPAERO for Mach 0.8 and a Reynolds number of 2.17 million with and without all the corrections. The differences between the simulation results of VSPAERO+TSD/IBL model with and without interference corrections are small. The computed results are compared to Run 378 wind tunnel data. While the lift coefficient is somewhat overpredicted. With all the corrections applied to the VSPAERO model for transonic viscous flow and wing-strut interference aerodynamics, the lift and drag coefficients match well to the wind tunnel data, although there is a small discrepancy in the drag polar at lower lift coefficients. The VSPAERO+TSD/IBL with the wing-strut interference correction model can be used as a fast and reliable tool for the TTBW aircraft conceptual analysis and design.

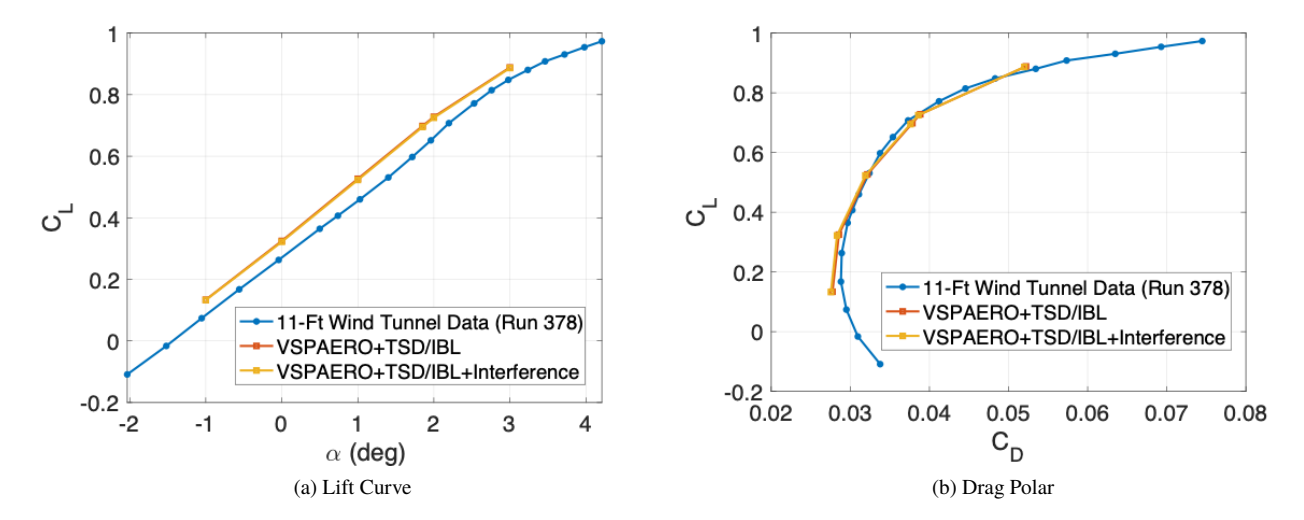


Figure 5 Mach 0.8 TTBW Lift Curve and Drag Polar at Mach 0.8 and  $Re = 2.17 \times 10^6$ 

## III. Structural Model of the Truss-Braced Wing

### A.Galerkin Method

A NASTRAN finite-element model (FEM) of the Mach 0.8TTBW is available from Boeing. The NASTRAN FEM comprises a detail structural model of the wing and struts, a shell structural model of the fuselage section that joins with the wing, and a beam-stick model of the rest of the fuselage and the tail empennage. This is shown in Figure 6. To reflect the estimated gross weights the fuel model in the Boeing NASTRAN model has been updated. The wing and strut root movements are set to zero for the cantilever wing model. The revised NASTRAN model is used to extract mode shapes for the aeroelastic analysis for the Mach 0.8 TTBW using the Galerkin method. Figure 7 shows the mode shapes of the first six modes.

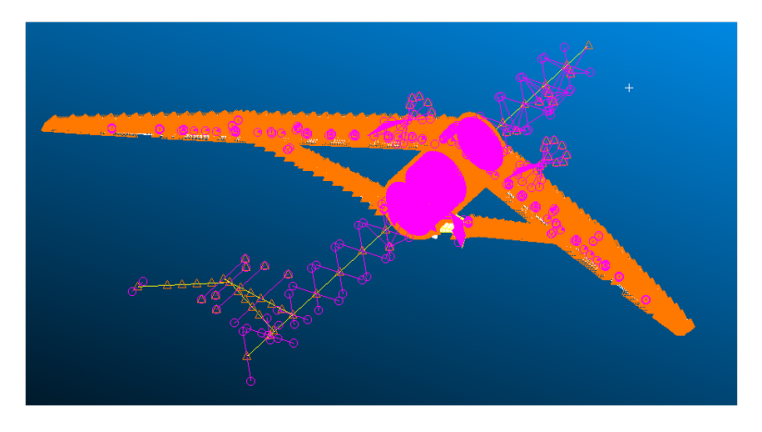
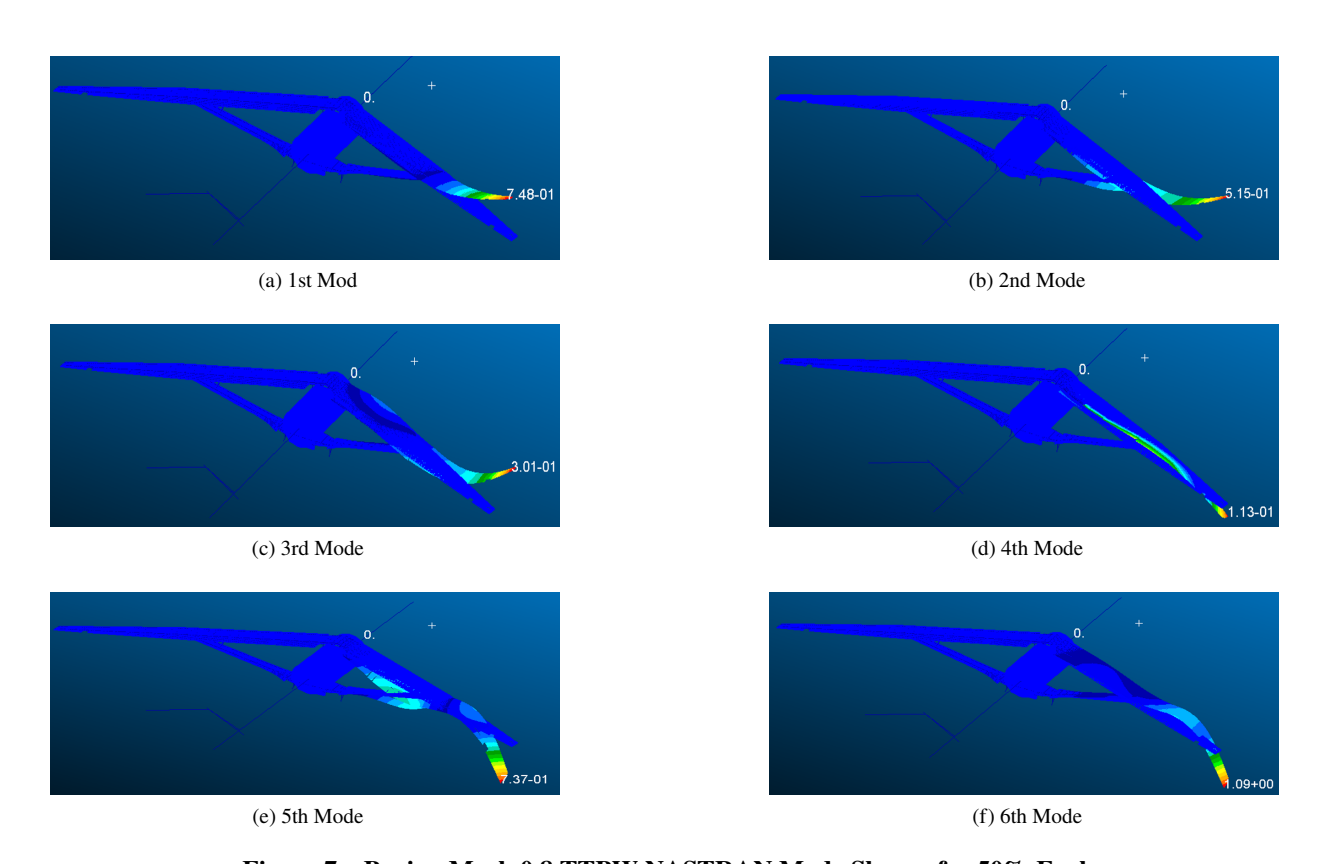


Figure 6 Boeing Mach 0.8 NASTRAN Finite-Element Model



 $Figure \ 7 \quad Boeing \ Mach \ 0.8 \ TTBW \ NASTRAN \ Mode \ Shapes \ for \ 50\% \ Fuel.$ 

The static structural equation can be written as

$$[K]U_a = F_a \tag{5}$$

where |K| is the stiffness matrix,  $U_a$  is the displacement vector, and  $F_a$  is the aerodynamic force vector. If the displacements are written as an expansion in terms of natural vibration modes  $\phi_i$ 

$$U_a = \sum_{i=1}^{N_{modes}} q_i \phi_i \tag{6}$$

where  $q_i$  are the generalized displacements. Substitution of the series representation into the structural equation and premultiplying by  $\phi^T$ , we obtain

$$\phi^T[K]\phi q = \phi^T F_a \tag{7}$$

where  $\phi^T[K]\phi$  is the diagonal generalized stiffness matrix and  $\phi^TF_a$  is the generalized aerodynamic force vector. After the generalized displacements q are calculated from the decoupled equations, the structural deformation due to aerodynamic force  $U_a$  can be obtained from Eq (2). The structural deformation due to the aircraft weight  $U_w$  is obtained from SOL 101 NASTRAN solution. Figure 8 shows the geometry deformation of the Mach 0.8 TTBW with 50% fuel under gravity load. The overall structural deformation can be calculated by

$$U = U_a + U_w \tag{8}$$

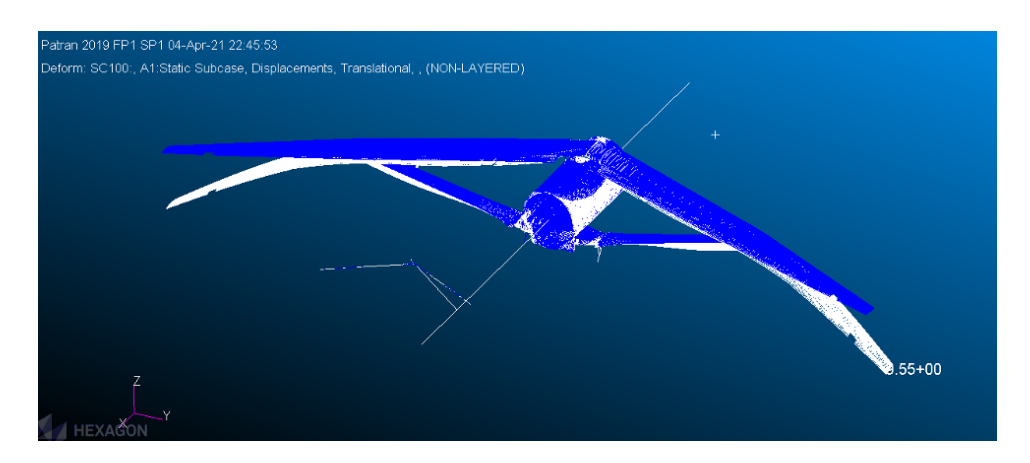


Figure 8 Mach 0.8 TTBW Structural Deformation Due to Gravity Load 50% Fuel.

## **B. Static Aeroelastic Analysis**

A basic schematic of the aeroelastic modeling strategy is depicted by Fig. 9. The VSPAERO model is couple to the mode shapes computed by NASTRAN using the Galerkin method to provide a rapid aero-structural analysis. At each iteration of the aeroelastic simulation the aerodynamic force  $F_z$  and moments  $M_x$  and  $M_y$  converted from wing sectional lift and pitching moment are applied to the Galerkin method.

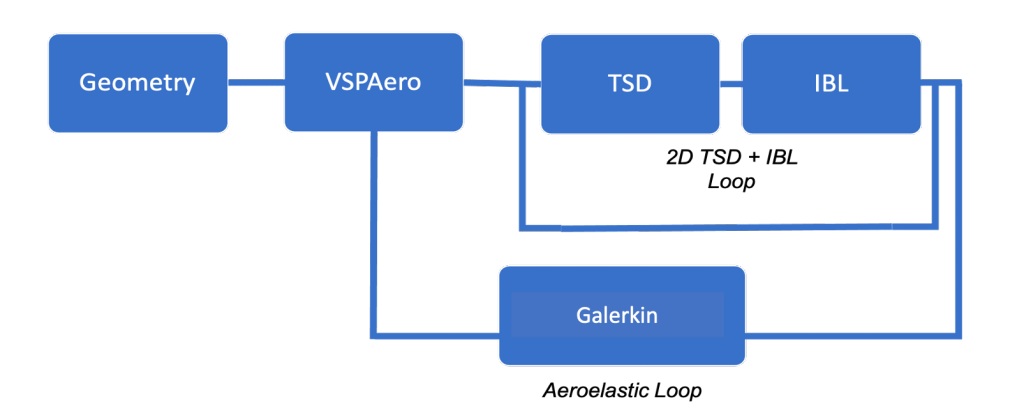


Figure 9 VSPAERO Aeroelastic Simulation Scheme Flow Chart

The wing coordinate system is shown in the following Fig. 10.

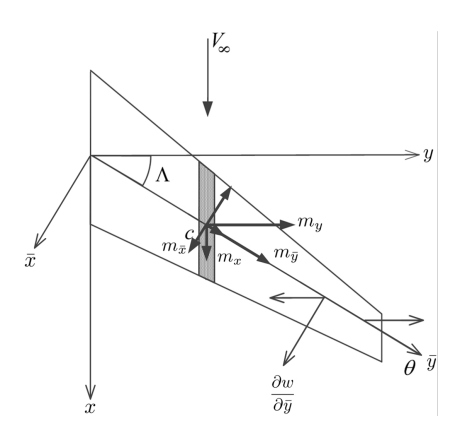


Figure 10 Wing Coordinate System

The distributed force and moments in the elastic axis coordinate system  $(\bar{x}, \bar{y}, z)$  due to aerodynamics are given by

$$f_z = c_l q_\infty c \cos \Lambda \tag{9}$$

$$m_{\bar{x}} = \left[ \left( c_{m_{\alpha c}} + c_{m_{x}} \tan \Lambda \right) q_{\infty} c^{2} + c_{l} q_{\infty} c e \right] \cos \Lambda \sin \Lambda \tag{10}$$

$$m_{\bar{y}} = \left[ \left( c_{m_{ac}} + c_{m_x} \tan \Lambda \right) q_{\infty} c^2 + c_l q_{\infty} c e \right] \cos^2 \Lambda \tag{11}$$

The hermite cubic interpolation function for the beam element in the finite-element method is

$$\mathbf{N}_{w}^{(i)^{\mathsf{T}}}(\bar{y}_{i}) = \begin{bmatrix} 1 - 3\left(\frac{\bar{y}_{i}}{l_{i}}\right)^{2} + 2\left(\frac{\bar{y}_{i}}{l_{i}}\right)^{3} \\ l_{i}\left[\frac{\bar{y}_{i}}{l_{i}} - 2\left(\frac{\bar{y}_{i}}{l_{i}}\right)^{2} + \left(\frac{\bar{y}_{i}}{l_{i}}\right)^{3}\right] \\ 3\left(\frac{\bar{y}_{i}}{l_{i}}\right)^{2} - 2\left(\frac{\bar{y}_{i}}{l_{i}}\right)^{3} \\ l_{i}\left[-\left(\frac{\bar{y}_{i}}{l_{i}}\right)^{2} + \left(\frac{\bar{y}_{i}}{l_{i}}\right)^{3}\right] \end{bmatrix}$$

$$(12)$$

$$\frac{d\mathbf{N}_{w}^{(i)^{\mathsf{T}}}(\bar{y}_{i})}{d\bar{y}} = \begin{bmatrix}
\frac{1}{l_{i}} \left[ -6\left(\frac{\bar{y}_{i}}{l_{i}}\right) + 6\left(\frac{\bar{y}_{i}}{l_{i}}\right)^{2}\right] \\
1 - 4\left(\frac{\bar{y}_{i}}{l_{i}}\right) + 3\left(\frac{\bar{y}_{i}}{l_{i}}\right)^{2} \\
\frac{1}{l_{i}} \left[ 6\left(\frac{\bar{y}_{i}}{l_{i}}\right) - 6\left(\frac{\bar{y}_{i}}{l_{i}}\right)^{2}\right] \\
-2\left(\frac{\bar{y}_{i}}{l_{i}}\right) + 3\left(\frac{\bar{y}_{i}}{l_{i}}\right)^{2}
\end{bmatrix}$$
(13)

The elemental force vector due to bending in the element coordinate system  $(\bar{x}, \bar{y}, z)$  is

$$\mathbf{F}_{w}^{(i)} = \begin{bmatrix} F_{z_{1}} \\ M_{\bar{x}_{1}} \\ F_{z_{2}} \\ M_{\bar{x}_{2}} \end{bmatrix} = \int_{0}^{l_{i}} \mathbf{N}_{w}^{(i)^{T}} (\bar{y}_{i}) \left( f_{z} + \frac{dm_{\bar{x}}}{d\bar{y}_{i}} \right) d\bar{y}_{i} = \int_{0}^{l_{i}} \mathbf{N}_{w}^{(i)^{T}} (\bar{y}_{i}) f_{z} d\bar{y}_{i} - \int_{0}^{l_{i}} \frac{d\mathbf{N}_{w}^{(i)^{T}} (\bar{y}_{i})}{d\bar{y}} m_{\bar{x}} d\bar{y}_{i}$$
(14)

The elemental force vector due to bending in the aircraft coordinate system (x, y, z) is

$$\mathbf{F}_{w}^{(i)} = \begin{bmatrix} F_{z_{1}} \\ M_{x_{1}} \\ M_{y_{1}} \\ F_{z_{2}} \\ M_{x_{2}} \\ M_{y_{2}} \end{bmatrix} = \begin{bmatrix} F_{z_{1}} \\ M_{\bar{x}_{1}} \cos \Lambda \\ -M_{\bar{x}_{1}} \sin \Lambda \\ F_{z_{2}} \\ M_{\bar{x}_{2}} \cos \Lambda \\ -M_{\bar{x}_{2}} \sin \Lambda \end{bmatrix}$$
(15)

The linear interpolation function for the rod element in the finite-element method is

$$\mathbf{N}_{\theta}^{(i)^{\top}}(\bar{\mathbf{y}}_i) = \begin{bmatrix} 1 - \frac{x_i}{l_i} \\ \frac{x_i}{l_i} \end{bmatrix}$$
 (16)

The elemental force vector due to torsion in the element coordinate system  $(\bar{x}, \bar{y}, z)$  is

$$\mathbf{F}_{\theta}^{(i)} = \begin{bmatrix} M_{\bar{y}_1} \\ M_{\bar{y}_2} \end{bmatrix} = \int_0^{l_i} \mathbf{N}_{\theta}^{(i)^{\mathsf{T}}} (\bar{y}_i) m_{\bar{y}} d\bar{y}_i$$

$$\tag{17}$$

The elemental force vector due to torsion in the aircraft coordinate system (x, y, z) is

$$\mathbf{F}_{\theta}^{(i)} = \begin{bmatrix} M_{x_1} \\ M_{y_1} \\ M_{x_2} \\ M_{y_2} \end{bmatrix} = \begin{bmatrix} M_{\bar{y}_1} \sin \Lambda \\ M_{\bar{y}_1} \cos \Lambda \\ M_{\bar{y}_2} \sin \Lambda \\ M_{\bar{y}_2} \cos \Lambda \end{bmatrix}$$
(18)

The total element force vector in the aircraft coordinate system (x, y, z) is

$$\mathbf{F}_{w}^{(i)} = \begin{bmatrix} F_{z_{1}} \\ M_{x_{1}} \\ M_{y_{1}} \\ F_{z_{2}} \\ M_{x_{2}} \\ M_{y_{2}} \end{bmatrix} = \begin{bmatrix} F_{z_{1}} \\ M_{\bar{x}_{1}} \cos \Lambda + M_{\bar{y}_{1}} \sin \Lambda \\ -M_{\bar{x}_{1}} \sin \Lambda + M_{\bar{y}_{1}} \cos \Lambda \\ F_{z_{2}} \\ M_{\bar{x}_{2}} \cos \Lambda + M_{\bar{y}_{2}} \sin \Lambda \\ -M_{\bar{x}_{1}} \sin \Lambda + M_{\bar{y}_{2}} \cos \Lambda \end{bmatrix}$$
(19)

The nodal forces on an element is shown in the following Fig. 11

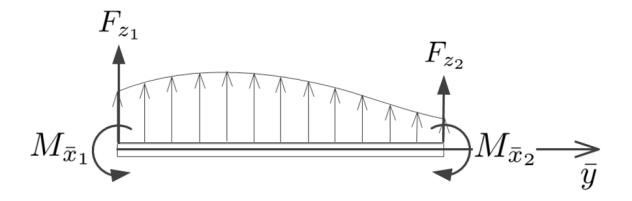


Figure 11 Wing Nodal Force Flow Chart

The Galerkin solution provides the structural deformation of the Mach 0.8 TTBW. Figure 12 shows the Mach 0.8 TTBW with 50% fuel wing bending displacement and twist at Mach 0.80, angle of attack  $2^{\circ}$ , and altitude 40,000ft. The results show a wing tip deflection 17.25 inches and twist down  $1.2^{\circ}$  at this condition.

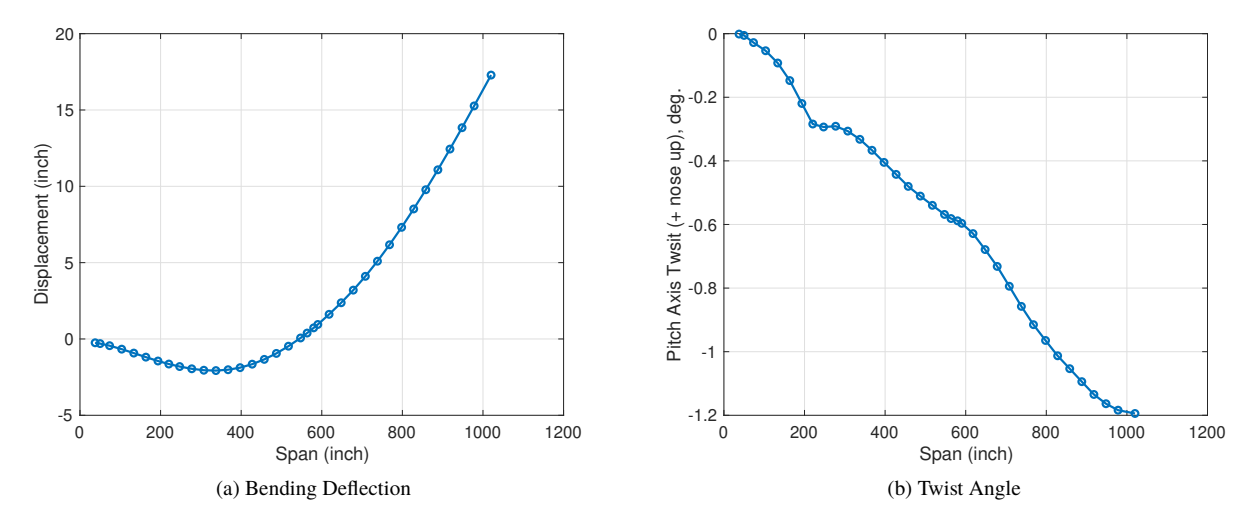


Figure 12 Mach 0.8 TTBW Wing Bending Deflection and Twist at  $M_{\infty} = 0.8$ ,  $\alpha = 2^{\circ}$ , and h = 40,000 ft

#### IV. FUN3D Aeroelastic Simulation

To validate the developed VSPAERO aeroelastic model, a validation study using high-fidelity CFD solver FUN3D is performed. FUN3D<sup>14,15</sup> solves the unsteady three-dimensional Navier-Stokes equations on mixed-element grids using a vertices-centered finite-volume method. Information exchange for flow computation on different partitions using multiple CPUs is implemented through the MPI (Message Passing Interface) protocol. It employs an implicit upwind algorithm in which the inviscid fluxes are obtained with a flux-difference-splitting scheme. At interfaces that delimits the neighboring control volumes, the inviscid fluxes are computed using an approximate Riemann solver based on the values on either side of the interfaces. The Roe flux difference splitting<sup>16</sup> is used in the current study. For second-order accuracy, the interface values are obtained by extrapolation of the control volume centroidal values, based on the gradients computed at the mesh vertices, using an unweighted least squares technique. The Venkatakrishnan<sup>17</sup> limiter is used in the current study to limit the reconstructed values when necessary. In this study, the tetrahedral mesh with prism layers is used. In FUN3D, for tetrahedral meshes, the full viscous fluxes are discretized using a finite-volume formulation in which the required velocity gradients on the dual faces are computed using the Green-Gauss theorem. The solution at each time-step is updated with a backward Euler time-differencing scheme. At each time step, the system of equations is approximately solved with either a multi-color point-implicit procedure or an implicit-line relaxation scheme. Local time-step scaling is employed to accelerate convergence to steady-state. To model turbulent flows, the one-equation model of Spalart-Allmaras<sup>18</sup> (S-A) is used in this study. The volume mesh is shown in Fig.13. The total number of the nodes for the mesh is about 96 million. The volume mesh is comprised of tetrahedral elements and a prism layer near the wall. The prism layer is used to resolve the turbulent boundary layer. The y+ of the first cell from the wall is less than 1.

The static aeroelastic simulation module in FUN3D is used for the aeroelastic simulation. The mode shapes are extracted from Boeing NASTRAN model with 50% fuel. Figure 14 shows the first six mode shapes which are interpolated from the NASTRAN mode shapes. Figure 15 shows the pressure coefficient contour on the Mach 0.8 TTBW surfaces at Mach 0.80, angle of attack  $2^{\circ}$ , and altitude 40,000ft. The Mach TTBW wing tip is deflected to the upward 17.3 inches and the shock wave on the wing surface turns weaker.

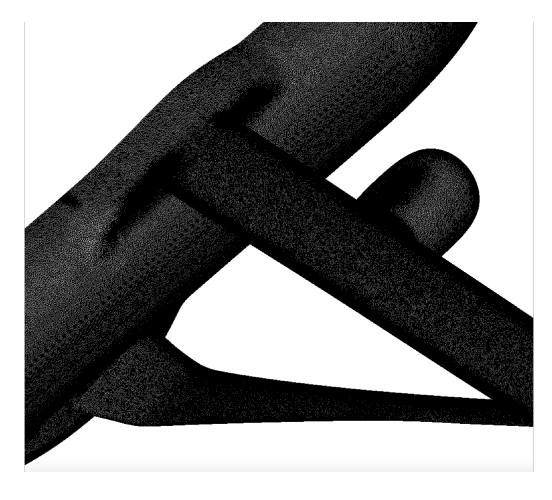


Figure 13 Close View of Mach 0.8 TTBW CFD Mesh

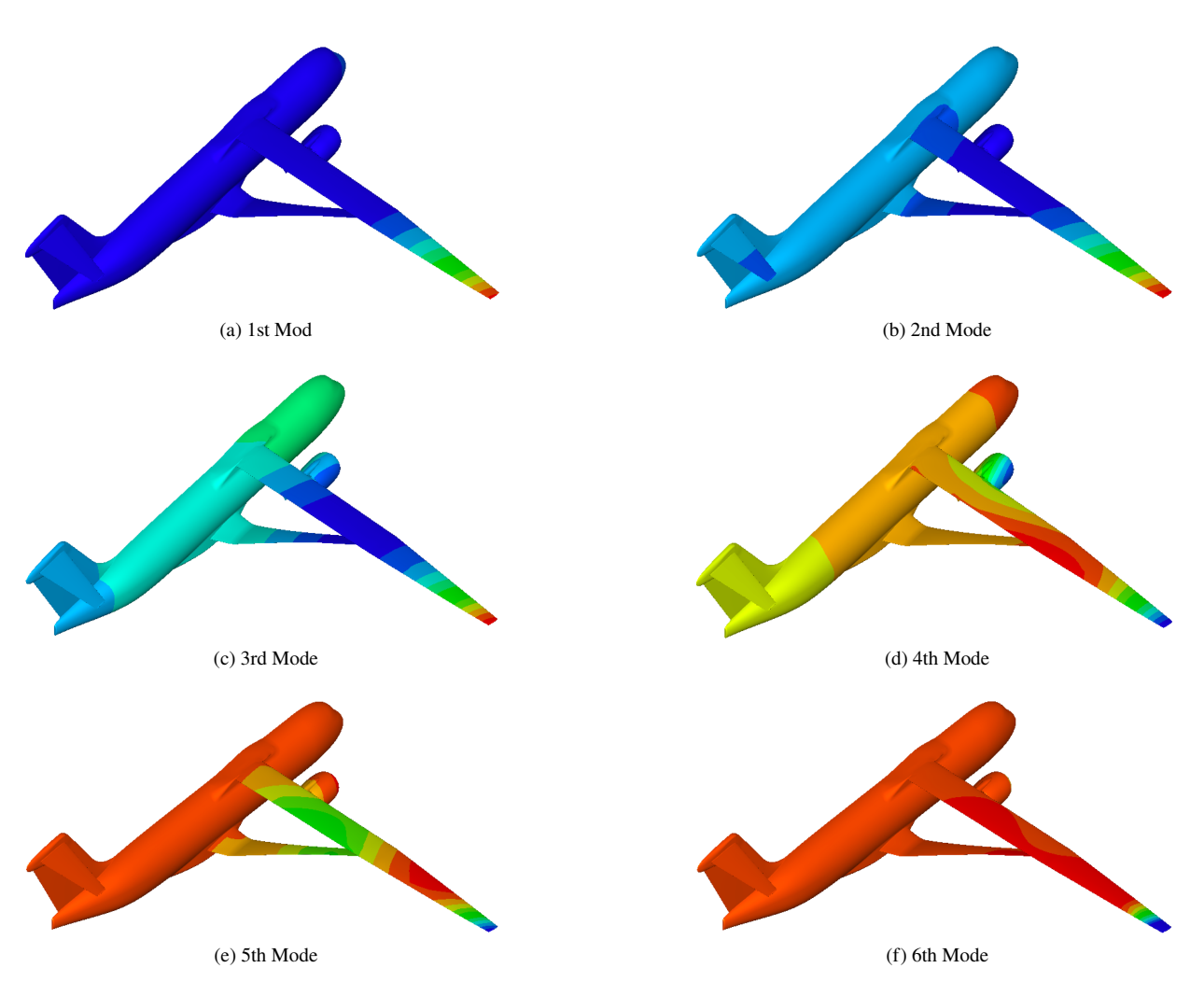


Figure 14 Mach 0.8 TTBW Mode Shapes for 50% Fuel.

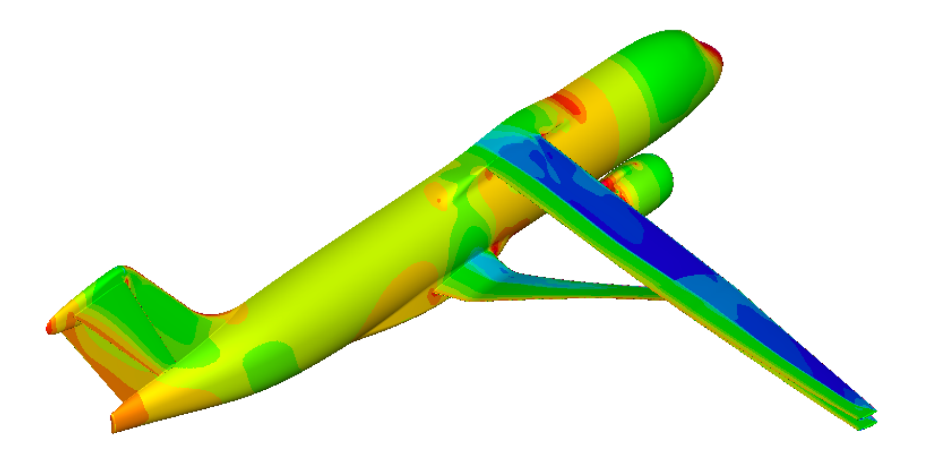


Figure 15 Pressure Coefficient Contour on the Mach 0.8 TTBW Surfaces at  $M_{\infty}=0.8$ ,  $\alpha=2^{\circ}$  and h = 40,000 ft

# V. TTBW Aeroelastic Simulation Results

The aero-structural analysis solver VSPAERO coupled to the mode shapes computed by NASTRAN using the Galerkin method is used to simulate the aeroelastic performance of the Mach 0.8 TTBW aircraft jig shape with 50% fuel. The VSPAERO results are compared with FUN3D simulation results. Figure 16 compares the lift, drag, pitch moment, and wing tip deflections calculated by the VSPAERO model and FUN3D for the Mach 0.8 TTBW aircraft jig shape with 50% fuel at Mach 0.8 and altitude 40,000 ft. The data calculated by the VSPAERO model show good agreement with the FUN3D simulation especially when the lift is less than 0.9. The discrepancy increases as the lift coefficient increases, which might be caused by a flow separation. The current VSPAERO model has some limitation in its ability to predict the flow separation, but overall the VSPAERO model demonstrates an good predictive capability at a much lower computational cost when compared to FUN3D aeroelastic simulations. The aeroelastic simulation results show that the aeroelastic lift coefficient is reduced about  $0.05 \sim 0.07$ , drag polar is not affected by aeroelasticity, and the pitching moment is reduced about 30% at Mach 0.8 and altitude 40,000 ft.

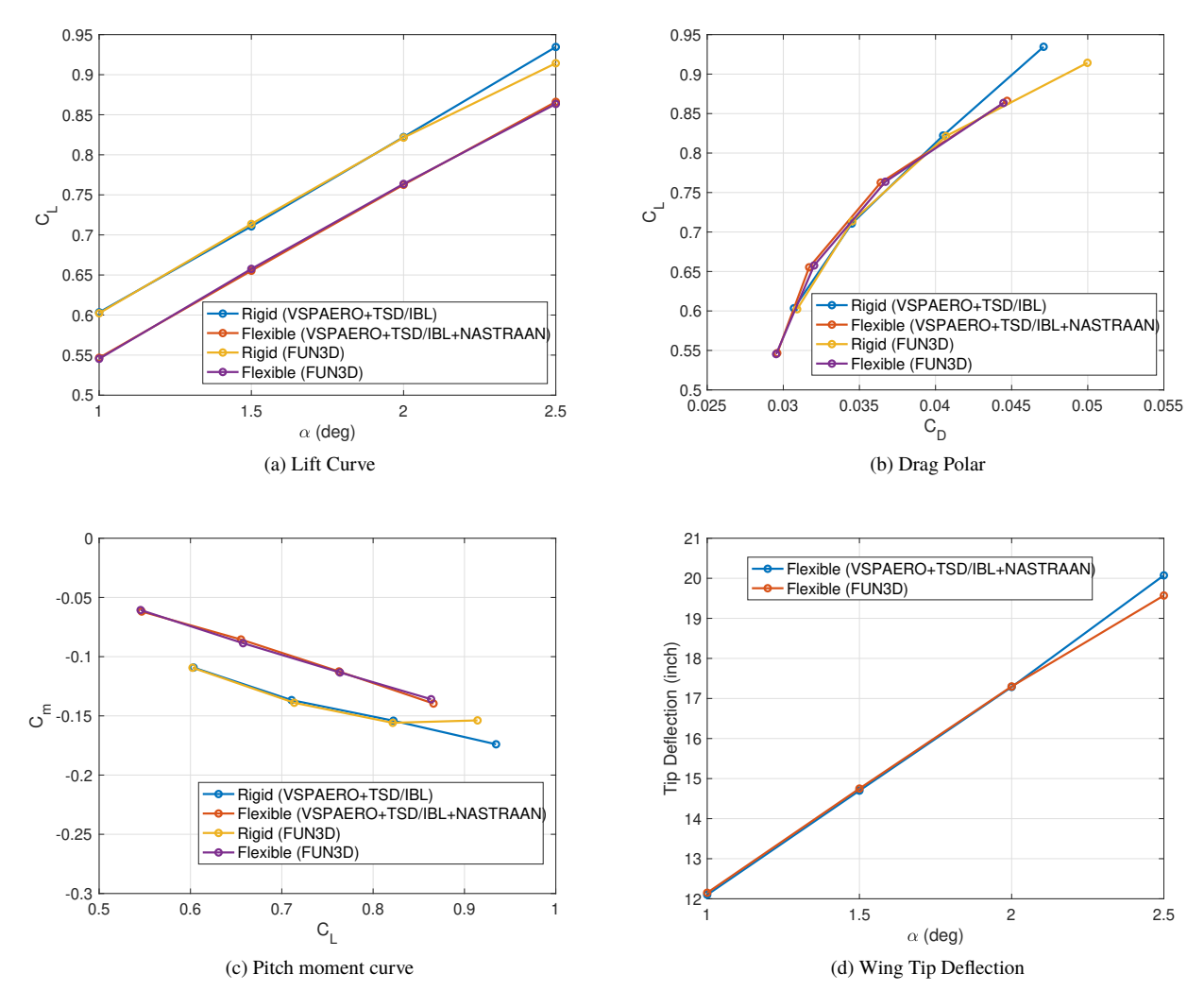


Figure 16 Mach 0.8 TTBW Aerodynamic Performance at  $M_{\infty} = 0.8$  and h = 40,000 ft.

## **Conclusions**

In this paper an aeroelastic analysis of the Mach 0.8 TTBW aircraft jig shape is performed using an in-house developed tool based on VSPAERO. A vortex-lattice model of the Mach 0.8 TTBW jig model is developed, and a transonic and viscous flow correction method is implemented in the VSPAERO models to account for transonic and viscous flow effects. A correction method for the wing-strut interference aerodynamics is developed and applied to the VSPAERO solver. The Galerkin method is used to calculate the geometry deformation under aerodynamic force. The developed aero-structural analysis solver VSPAERO coupled to the mode shapes computed by NASTRAN using the Galerkin method provides a rapid aircraft aero-structural analysis. A high-fidelity CFD solver FUN3D is used to verify the results. The aeroelastic simulation results indicate that the aeroelastic lift coefficient is reduced about  $0.05 \sim 0.07$ , drag polar is not affected by aeroelasticity, and the pitching moment is reduced about 30% at Mach 0.8 and altitude 40,000 ft.

# Acknowledgment

The authors wish to acknowledge NASA Advanced Air Transport Technology project for the funding support of this work. The authors also acknowledge Boeing Research and Technology and in particular Christopher Droney, Neal Harrison, Michael Beyar, Eric Dickey, and Anthony Sclafani, along with the NASA technical POC, Gregory Gatlin, for their research conducted under the NASA BAART contracts NNL10AA05B and NNL16AA04B. The research published in this paper is made possible by the technical data and wind tunnel test data furnished under these BAARTcontracts.

#### References

- <sup>1</sup> Bhatia, M., et. al.. "Structural and Aeroelastic Characteristics of Truss-Braced Wing: A Parametric Study," Journal of Aircraft, Vol 49, No. 1, 2012.
- <sup>2</sup> Gundlach, J. F., Tetrault, P. A., Gern, F. H., Nagshineh-Pour, A. H., Ko, A., Schetz, J. A., et. al., "Conceptual Design Studies of a Strut-Braced Wing Transonic Transport," Journal of Aircraft, Vol. 37, No. 6, 2000.
- <sup>3</sup> Gur, O., Bhatia, M., Schetz, J.A., Mason, W. H., Kapania, R. K., and Mavris, D. N., "Design Optimization of a Truss-Braced Wing Transport Aircraft," Journal of Aircraft, Vol. 47, No. 6, 2010.
- <sup>4</sup> Harrison, N. A., Beyar, M. D., Dickey, E. D., Hoffman, K., Gatlin, G.M. and Viken, S. A., "Development of an Efficient Mach=0.80 Transonic Truss-Braced Wing Aircraft," AIAA SciTech Conference, AIAA-2020-0011, January 2020.
- <sup>5</sup> Litherland B. and Rieth K., "VSP Aircraft Analysis User Manual,", July. 2014
- <sup>6</sup> Fujiwara, G., Chaparro, D., and Nguyen, N., "An Integral Boundary Layer Direct Method Applied to 2D Transonic Small-Disturbance Equations," 34th AIAA Applied Aerodynamics Conference, AIAA-2016-3160, June 2016.
- <sup>7</sup> Chaparro, D., Fujiwara, G., Ting, E., and Nguyen, N., "Aerodynamic Modeling of Transonic Aircraft Using Vortex Lattice Coupled with Transonic Small Disturbance for Conceptual Design," 34th AIAA Applied Aerodynamics Conference, AIAA-2016-3012, June 2016.
- <sup>8</sup> Chaparro, D., Fujiwara, G. E., Ting, E., and Nguyen, N. T., "Transonic and Viscous Potential Flow Method Applied to Flexible Wing Transport Aircraft," 35th AIAA Applied Aerodynamics Conference, AIAA-2017-4221, June 2017.
- <sup>9</sup> Stahara, S. S., "Operational Manual for Two-Dimensional Transonic Code TSFOIL," NASA Contractor Report 3064, December, 1978.
- <sup>10</sup> Drela, M., "A User's Guide to MSES 3.05," MIT Department of Aeronautics and Astronautics, July 2007.
- <sup>11</sup> Fugate, J., Nguyen, N., and Xiong, J., "Aero-Structural Modeling of the Truss-BracedWing Aircraft Using Potential Method with Correction Methods for Transonic Viscous Flow and Wing-Strut Interference Aerodynamics," AIAA Aviation Conference, AIAA-2019-3028, June 2019.
- <sup>12</sup> Xiong, J., Nguyen, N., and Fugate, J., "Investigation of Truss-Braced Wing Aircraft Transonic Wing-Strut Interference Effects Using FUN3D," AIAA Aviation Conference, AIAA-2019-3026, June 2019.
- <sup>13</sup> Xiong, J., Nguyen, N., and Fugate, J., "Study of Mach 0.8 Transonic Truss-Braced Wing Aircraft Wing-Strut Interference Effects," AIAA SciTech Conference, AIAA-2020-0336, January 2020.
- <sup>14</sup> Biedron, R. T., et al., "FUN3D Manual 13.2,", NASA TM-2017-219661, Aug. 2017
- <sup>15</sup> Lee-Rausch, E. M., Hammond, D. P., Nielsen, E. J., Pirzadeh, S. Z., and Rumsey, C. L., "Application of the FUN3D Unstructured-Grid Navier-Stokes Solver to the 4th AIAA Drag Prediction Workshop cases," AIAA Aviation Conference, AIAA-2010-4511, January 2019.
- <sup>16</sup> Roe, P. L., "Approximate Riemann Solvers, Parameter Vectors and Difference Schemes,", Journal of Computational Physics, Vol. 46, No. 2, 1980, pp. 357-378
- <sup>17</sup> Venkatakrishnan, V., "Convergence to Steady State Solutions of the Euler Equations on Unstructured Grids with Limiters,", Journal of Computational Physics, Vol. 118, No. 1, 1995, pp. 120-130
- <sup>18</sup> Spalart, P. R. and Allmaras, S. R., "A One-Equation Turbulence Model for Aerodynamic Flows," AIAA Science and Technology Forum and Exposition, AIAA-1992-0439, January 1992.